Preprints of the 19th World Congress
The International Federation of Automatic Control
Cape Town, South Africa. August 24-29, 2014

Offset-Free Model Predictive Control for Output Voltage Regulation of Three-Phase Inverter for Uninterruptible Power Supply Applications ⋆

Seok-Kyoon Kim *, **Chang Reung Park** **, **Young Il Lee** ***

* *Research Institute of EIT, SeoulTech., Seoul, Korea. (e-mail: lotus45kr@gmail.com).*
** *Department of EIE, SeoulTech.,Seoul, Korea. (e-mail: jhon316@seoultech.ac.kr)*
*** *Department of EIE, SeoulTech.,Seoul, Korea. (e-mail: yilee@seoultech.ac.kr, the corresponding author)*

Abstract: This paper proposes an offset-free model predictive control (MPC) method for output voltage regulation of the three phase inverter for an uninterruptible power supply (UPS) application. A use of a disturbance observer (DOB) is made to estimate the unknown disturbance caused by the load current and a plant-model mismatch. The proposed MPC optimizes the one step ahead cost function. The online computation considering the input constraint of the inverter system is very simple. It is shown that the closed-loop system is globally asymptotically stable in the presence of input constraints and that the integral action in the DOB eliminates the steady state errors caused by a plant-model mismatch. The effectiveness of the closed-loop system is experimentally shown under a use of resistive load.

1. INTRODUCTION

It is important for three phase uninturruptible power supply (UPS) applications to regulate the output voltage while keeping other state variables bounded in the presence of input constraints. Conventionally, the output voltage of the three phase UPS system is controlled under the cascade control strategy which is comprised of the current (inner) and voltage (outer) loops Loh et al. [2003], Kassakian et al. [1991], Mohan et al. [1995], Abdel-Rahim and Quaicoe [1996], Kawabata et al. [1990], Ito and Kawauchi [1995], Cho et al. [2012], Lee et al. [2001a,b], Willmann et al. [2007], Kim et al. [2014]. Since the current controller for the inner-loop plays the pivotal role for the closed-loop performance, various control strategies such as proportional-integral (PI) Loh et al. [2003], Kassakian et al. [1991], Mohan et al. [1995], Abdel-Rahim and Quaicoe [1996], deadbeat Kawabata et al. [1990], Ito and Kawauchi [1995], Cho et al. [2012], H_∞ Lee et al. [2001a], Willmann et al. [2007], and μ-synthesis Lee et al. [2001b] were applied. On the other hand, the output voltage controller in the outer-loop was designed through the classical PI scheme. The PI controllers Loh et al. [2003], Kassakian et al. [1991], Mohan et al. [1995], Abdel-Rahim and Quaicoe [1996] and deadbeat controllers Kawabata et al. [1990], Ito and Kawauchi [1995], Cho et al. [2012] did not ensure the closed-loop stability in the presence of input constraints. Although H_∞ Lee et al. [2001a], Willmann et al. [2007] and μ-synthesis Lee et al. [2001b] methods did consider the input constraint, the stability analysis result is just local.

Recently, in the applications of the power electronics, there have been several model predictive control (MPC) schemes for regulation of target variables in the presence of input constraint via optimizing a cost function such as the finite control set (FCS)-MPC Vargas et al. [2007], Cortes et al. [2010, 2009] and the explicit MPC Mariethoz and Morari [2009]. In the case of FCS-MPC Vargas et al. [2007], Cortes et al. [2010, 2009], they does not require any use of the pulse-width modulation (PWM) techniques. This control structure is very simple to be implemented; nevertheless, this type MPCs optimize a cost function of the tracking error at each time through the exhaustive search method. However, there was no convergence analysis. The explicit MPC scheme in Mariethoz and Morari [2009] seems to make up for these weak points in the FCS-MPC Vargas et al. [2007], Cortes et al. [2010, 2009] using the multi-parametric programming as in Bemporad et al. [2002], Borrelli [2003]. They, however, require lots of off-line optimization such as partitioning the state space, and should perform a lot of online membership tests to determine the location of the state variables. The load of online membership tests might be increased significantly as the state space is finely partitioned.

This paper proposes a new MPC strategy by compensating for the weak points of the previous contributions. Because the proposed control scheme is designed following a multi-variable design approach in discrete-time state space, the extra outer-loop controller is not required unlike classical cascade approaches using the PI controllers Loh et al. [2003], Kassakian et al. [1991], Mohan et al. [1995],

⋆ This work was supported by the National Research Foundation of Korea (NRF) grants funded by the Korea government (MEST) (No. 2011-0029233)

Abdel-Rahim and Quaicoe [1996], the deadbeat controllers Kawabata et al. [1990], Ito and Kawauchi [1995], Cho et al. [2012], and the optimal state-feedback controllers Lee et al. [2001a,b], Willmann et al. [2007]. Specifically, a Luenberger type disturbance observer (DOB) is designed to estimate the disturbance comprising the unknown load current and a plant-model mismatch, and an MPC is designed in such a way that a one step head cost function of the error state is minimized without any use of numerical methods. Thereafter, it is shown that the closed-loop system is global asymptotic stable in the presence of inherent input constraints and that the integral action in the DOB gets rid of an offset error caused by a plant-model mismatch. The experimental results show that the closed-loop performance is satisfactory under use of a resistive load. This paper is organized as follows: Section 2 introduces the mathematical model of the three-phase inverter with a LC filter in the rotational frame. Section 3 designs a DOB in order to estimate the disturbance caused by a plant-model mismatch. Section 4 devises an MPC scheme and analyzes the closed-loop stability. Section 5 shows the effectiveness of the proposed MPC scheme by performing the experiments. Section 6 concludes this paper.

2. SYSTEM DESCRIPTION AND MATHEMATICAL MODEL IN *D-Q* FRAME

This paper considers a three-phase UPS system comprising a three-phase inverter and a load depicted in Fig. 1 Willmann et al. [2007], Lim and Lee [2012]. In this

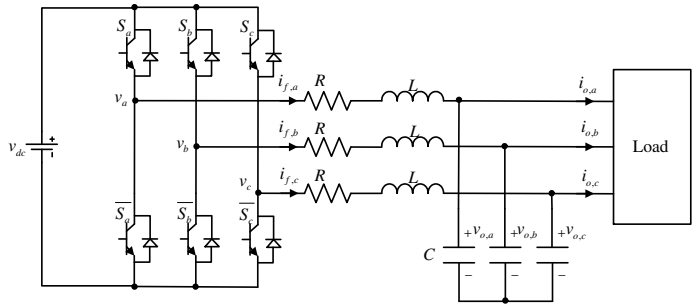

Fig. 1. The UPS system topology

system, the DC-link voltage V_{dc} is regarded as an ideal voltage source since it normally has low impedance. Then, applying Kirchoff's law to this system and the standard *d-q* transformation, we have following state equation for the UPS system depicted in Figure 1:

$$\frac{d\mathbf{x}(t)}{dt} = A_c\mathbf{x}(t) + B_c\mathbf{u}(t) + B_{dc}\mathbf{i}_o(t), \tag{1}$$

$$\mathbf{x}(t) := \begin{bmatrix} \mathbf{i}_f(t) \\ \mathbf{v}_c(t) \end{bmatrix},\ A_c := \begin{bmatrix} A_{c,11} & A_{c,12} \\ A_{c,21} & A_{c,22} \end{bmatrix},\ B_c := \begin{bmatrix} \frac{1}{L}I_{2\times 2} \\ 0_{2\times 2} \end{bmatrix},$$

$$A_{c,11} := \begin{bmatrix} -\alpha & \omega \\ -\omega & -\alpha \end{bmatrix},\ A_{c,12} := -\frac{1}{L}I_{2\times 2},\ A_{c,21} := \frac{1}{C}I_{2\times 2},$$

$$A_{c,22} := \begin{bmatrix} 0 & \omega \\ -\omega & 0 \end{bmatrix},\ B_{dc} := \begin{bmatrix} 0_{2\times 2} \\ -\frac{1}{C}I_{2\times 2} \end{bmatrix},\ \alpha := \frac{R}{L},$$

$I_{2\times 2}$ and $0_{2\times 2}$ denote 2×2 dimensional identity and zero matrices, respectively, and ω denotes the frequency of AC output voltage. Note that the control input $\mathbf{u}(t)$ can be viewed as a continuous signal, i.e., $\mathbf{u}(t) \in \Re^2$, $\forall t$, since the switches S_x of the inverter are controlled by a PWM method with a high sampling frequency Cortes et al. [2009]. Note that the matrix A_c is stable for any $R > 0$, $L > 0$, and $C > 0$. i.e., the real parts of the all eigenvalues of A_c are negative. The input voltages $v_d(t)$ and $v_q(t)$ in the *d-q* frame should be constrained in the hexagon U_{hex} defined by

$$U_{hex} := \Big\{ \mathbf{u} \in \Re^2 \ \Big|\ |\frac{3}{2}u_1 + \frac{\sqrt{3}}{2}u_2| \le V_{dc},\ \sqrt{3}|u_2| \le V_{dc},$$
$$|-\frac{3}{2}u_1 + \frac{\sqrt{3}}{2}u_2| \le V_{dc} \Big\}. \tag{2}$$

In order to simply the design procedure of the MPC, the following input constraint set is taken into account instead of U_{hex}:

$$U_c := \Big\{ \mathbf{u} \in \Re^2 \ \Big|\ \|\mathbf{u}\| \le \frac{V_{dc}}{\sqrt{3}} \Big\}. \tag{3}$$

Since U_c is the largest circle contained in the set U_{hex}, it is qualified as a satisfactory approximation. These two sets are depicted in Fig. 2. The continuous-time state equation

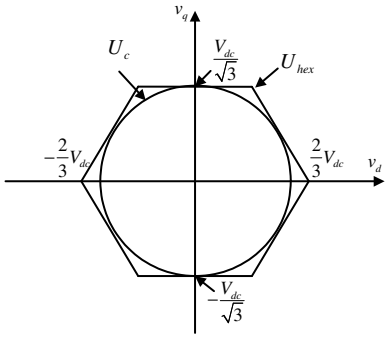

Fig. 2. Input constraint set U_{hex} and U_c

(1) can be transformed to the following discrete-time state equation with the sampling time $h > 0$:

$$\mathbf{x}(k+1) = A\mathbf{x}(k) + B\mathbf{u}(k) + B_d\mathbf{i}_o(k), \tag{4}$$

where

$$\mathbf{x}(k) := \begin{bmatrix} \mathbf{i}_f(k) \\ \mathbf{v}_c(k) \end{bmatrix},\ \mathbf{i}_f(k) := \begin{bmatrix} i_{f,d}(k) \\ i_{f,q}(k) \end{bmatrix},$$

$$\mathbf{v}_c(k) := \begin{bmatrix} v_{c,d}(k) \\ v_{c,q}(k) \end{bmatrix},\ \mathbf{u}(k) := \begin{bmatrix} v_d(k) \\ v_q(k) \end{bmatrix},$$

$$A := e^{A_c h} = \begin{bmatrix} A_{11} & A_{12} \\ A_{21} & A_{22} \end{bmatrix},\ B := \int_0^h e^{A_c\tau}d\tau B_c = \begin{bmatrix} B_1 \\ B_2 \end{bmatrix},$$

$$B_d := \int_0^h e^{A_c\tau}d\tau B_{d,c} = \begin{bmatrix} B_{d,1} \\ B_{d,2} \end{bmatrix},\ \mathbf{i}_o(k) := \begin{bmatrix} i_{o,d}(k) \\ i_{o,q}(k) \end{bmatrix}.$$

Note that matrix A of the discrete time system (4) is also stable since matrix A_c of the continuous time system (1) is stable for any $R > 0$, $L > 0$, and $C > 0$. Moreover, because the load current $\mathbf{i}_o(k)$ is sufficiently slower than

the state $\mathbf{x}(k)$, it is reasonable to assume that the load current $\mathbf{i}_o(k)$ can be treated as a constant. i.e.,

$$\mathbf{i}_o(k+1) \approx \mathbf{i}_o(k),\ \forall k. \tag{5}$$

For details of the validity of the assumption (5), see Cortes et al. [2009]. An MPC is devised based on the discrete-time model (4) through the following two sections.

3. DOB DESIGN

This section designs a DOB to estimate the unknown load current $\mathbf{i}_o(k)$ which is assumed to be an unknown constant as in Cortes et al. [2009]. Considering the discrete time system (4), construct the DOB as follows:

$$\begin{aligned}\hat{\mathbf{x}}(k+1) &= A\hat{\mathbf{x}}(k) + B_d\hat{\mathbf{i}}_o(k) + B\mathbf{u}(k) \\ &\quad + L_1(\mathbf{x}(k) - \hat{\mathbf{x}}(k)), \qquad (6)\\ \hat{\mathbf{i}}_o(k+1) &= \hat{\mathbf{i}}_o(k) + L_2(\mathbf{x}(k) - \hat{\mathbf{x}}(k)), \qquad (7)\end{aligned}$$

where L_1 and L_2 denote the DOB gain. Defining $\mathbf{z}(k) := [\,\mathbf{x}(k)\ \mathbf{i}_o(k)\,]^T$, $\hat{\mathbf{z}}(k) := [\,\hat{\mathbf{x}}(k)\ \hat{\mathbf{i}}_o(k)\,]^T$, and $\mathbf{e}_z(k) := \mathbf{z}(k) - \hat{\mathbf{z}}(k)$, we have the following error dynamics by subtracting (6) and (7) from (4) and (5), respectively,

$$\mathbf{e}_z(k+1) = A_{obs}\mathbf{e}_z(k), \tag{8}$$

where

$$A_{obs} := A_a - L_{obs}C_a,\ A_a := \begin{bmatrix} A & B_d \\ 0_{2\times4} & I_{2\times2}\end{bmatrix},$$
$$C_a := [\,I_{4\times4}\ 0_{4\times2}\,],\ L_{obs} := \begin{bmatrix} L_1 \\ L_2\end{bmatrix}.$$

Note that it can be shown that the pair (A_a, C_a) is observable provided that matrix B_d has full column rank. It means that there exists L_{obs} such that $(A_a - L_{obs}C_a)$ is stable. i.e., the all eigenvalues of matrix $A_{obs} = A_a - L_{obs}C_a$ are located within the unit circle.

4. OFFSET-FREE MPC DESIGN

In this section, an MPC scheme will be designed so that

$$\lim_{k\to\infty} \mathbf{v}_c(k) = \mathbf{v}_c^*(r), \tag{9}$$

while satisfying the input constraint. Section 4-1 derives a steady state condition for the the closed-loop system. In Section 4-2, an MPC solution is analytically found by solving a constrained optimization problem. Section 4-3 shows that the closed-loop system is globally asymptotically stable in the presence of input constraints. Section 4-4 proves that the integral action of the DOB eliminates the steady state error caused by a plant-model mismatch.

4.1 A steady state condition

Consider the steady state equation of the system (4) given by

$$\mathbf{x}^0 = A\mathbf{x}^0 + B\mathbf{u}^0 + B_d\mathbf{i}_o, \tag{10}$$

where $\mathbf{x}^0 := [\,\mathbf{i}_f^0\ \mathbf{v}_c^0\,]^T$ and $\mathbf{u}^0$ denote the steady state values of the state $\mathbf{x}(k)$ and the control $\mathbf{u}(k)$, respectively, and $\mathbf{i}_f^0$ and $\mathbf{v}_c^0$ present the steady state value of $\mathbf{i}_f(k)$ and $\mathbf{v}_c(k)$, respectively. In order to achieve the control objective (9), the constraint $\mathbf{v}_c^0 = \mathbf{v}_c^*(r)$ must be imposed to the equation (10). Then, rearranging the equation (10), it is easy to verify that the steady state values of the inductor current and the control input are uniquely determined as

$$\begin{bmatrix}\mathbf{i}_f^0(r,\mathbf{i}_o)\\ \mathbf{u}^0(r,\mathbf{i}_o)\end{bmatrix} = \begin{bmatrix}Z_{1,1}\\ Z_{1,2}\end{bmatrix}\mathbf{v}_c^*(r) + \begin{bmatrix}Z_{2,1}\\ Z_{2,2}\end{bmatrix}\mathbf{i}_o, \tag{11}$$

where

$$\begin{bmatrix}Z_{1,1}\\ Z_{1,2}\end{bmatrix} := \begin{bmatrix}I_{2\times2} - A_{11} & -B_1\\ -A_{21} & -B_2\end{bmatrix}^{-1}\begin{bmatrix}A_{12}\\ A_{22} - I_{2\times2}\end{bmatrix},$$
$$\begin{bmatrix}Z_{2,1}\\ Z_{2,2}\end{bmatrix} := \begin{bmatrix}I_{2\times2} - A_{11} & -B_1\\ -A_{21} & -B_2\end{bmatrix}^{-1}B_d,$$
$$A = \begin{bmatrix}A_{11} & A_{12}\\ A_{21} & A_{22}\end{bmatrix},\ B = \begin{bmatrix}B_1\\ B_2\end{bmatrix}.$$

Moreover, it is obvious that the corresponding steady state control $\mathbf{u}^0(r,\mathbf{i}_o)$ must satisfy that

$$\mathbf{u}^0(r,\mathbf{i}_o) \in U_c. \tag{12}$$

Hence, it turns out that the capacitor voltage reference r is valid if the corresponding steady state control $\mathbf{u}^0(r,\mathbf{i}_o)$ satisfies the condition (12). For the rest of the paper, the voltage reference r is said to be admissible when the corresponding steady state control $\mathbf{u}^0(r,\mathbf{i}_o) \in U_c$.

4.2 MPC design

In this section, using the DOB (6)-(7), an MPC is designed such that the output voltage $\mathbf{v}_c(k)$ converges to its reference $\mathbf{v}_c^*(r)$ while fulfilling input constraints. To this end, defining the error state as $\mathbf{e}(k) := \mathbf{x}(k) - \mathbf{x}^0(r,\mathbf{i}_o)$, it holds that

$$\begin{aligned}\mathbf{e}(k+1|k) &= \mathbf{x}(k+1) - \mathbf{x}^0(r,\mathbf{i}_o)\\ &= A\mathbf{x}(k) + B\mathbf{u}(k) + B_d\mathbf{i}_o - \mathbf{x}^0(r,\mathbf{i}_o). \qquad (13)\end{aligned}$$

Note that, since the load current $\mathbf{i}_o$ is unavailable, so is $\mathbf{x}^0(r,\mathbf{i}_o)$. Hence, it is impossible to use the predicted error state $\mathbf{e}(k+1|k)$ generated by the equation (13). Thus, we modify the equation (13) as follows:

$$\hat{\mathbf{e}}(k+1|k) = A\mathbf{x}(k) + B\mathbf{u}(k) + B_d\hat{\mathbf{i}}_o(k) - \hat{\mathbf{x}}^0(r,k), \tag{14}$$

where

$$\hat{\mathbf{x}}^0(r,k) := \mathbf{x}^0(r,\mathbf{i}_o)\Big|_{\mathbf{i}_o=\hat{\mathbf{i}}_o(k)} = \begin{bmatrix}\hat{\mathbf{i}}_f^0(r,k)\\ \mathbf{v}_c^*(r)\end{bmatrix},\ \forall k, \tag{15}$$

$$\hat{\mathbf{i}}_f^0(r,k) := \mathbf{i}_f^0(r,\mathbf{i}_o)\Big|_{\mathbf{i}_o=\hat{\mathbf{i}}_o(k)} = Z_{1,1}\mathbf{v}_c^*(r) + Z_{2,1}\hat{\mathbf{i}}_o(k),\ \forall k, \tag{16}$$

and $\hat{\mathbf{i}}_o(k)$ denotes the load current estimates generated by the DOB (6)-(7). Using the equation (14), the cost function is constructed as

$$J(\mathbf{x}(k),\hat{\mathbf{i}}_o(k),\mathbf{u}(k)) := \|\hat{\mathbf{e}}(k+1|k)\|_P^2 + r_u\|\hat{\mathbf{e}}_u(k)\|^2, \tag{17}$$

where $\hat{\mathbf{e}}_u(k) := \mathbf{u}(k) - \hat{\mathbf{u}}^0(r,k)$,

$$\hat{\mathbf{u}}^0(r,k) := \mathbf{u}(r,\mathbf{i}_o)\Big|_{\mathbf{i}_o=\hat{\mathbf{i}}_o(k)} = Z_{1,2}\mathbf{v}_c^*(r) + Z_{2,2}\hat{\mathbf{i}}_o(k), \quad (18)$$

$\|\cdot\|_{\mathcal{A}}^2$ is defined as $\|\cdot\|_{\mathcal{A}}^2 := (\cdot)^T\mathcal{A}(\cdot)$ for a given square matrix $\mathcal{A}$, and $r_u > 0$ and $P = P^T > 0$ are design parameters. The corresponding optimization problem is given by:

$$\min_{\mathbf{u}(k)\in U_c} J(\mathbf{x}(k), \hat{\mathbf{i}}_o(k), \mathbf{u}(k)). \quad (19)$$

In order to find the MPC explicitly, rewrite the cost function (17) as

$$\begin{aligned} J(\mathbf{x}(k), \hat{\mathbf{i}}_o(k), \mathbf{u}(k)) = {} & \mathbf{u}^T(k)(B^TPB + r_uI)\mathbf{u}(k) \\ & + 2\mathbf{u}^T(k)(B^TP\mathbf{w}(k) - r_u\hat{\mathbf{u}}^0(r,k)) \\ & + \|\mathbf{w}(k)\|^2 + r_u\|\hat{\mathbf{u}}^0(r,k)\|^2, \end{aligned} \quad (20)$$

where $\mathbf{w}(k) := A\mathbf{x}(k) + B_d\hat{\mathbf{i}}_o(k) - \hat{\mathbf{x}}^0(r,k)$. Let $\mathbf{u}_{uc}^*(k)$ be the unconstrained optimizer of the problem (19). Then, the unconstrained optimizer $\mathbf{u}_{uc}^*(k)$ is obtained by solving $\dfrac{\partial J(\mathbf{x}(k), \hat{\mathbf{i}}_o(k), \mathbf{u}(k))}{\partial \mathbf{u}(k)} = \mathbf{0}$:

$$\mathbf{u}_{uc}^*(k) = -(B^TPB + r_uI)^{-1}(B^TP\mathbf{w}(k) - r_u\hat{\mathbf{u}}^0(r,k)).$$

Hence, it is obvious that the constrained optimizer $\mathbf{u}^*(k)$ of the problem (19) is equal to the unconstrained one $\mathbf{u}_{uc}^*(k)$ if $\mathbf{u}_{uc}^*(k) \in U_c$. Whereas, if $\mathbf{u}_{uc}^*(k) \notin U_c$, the optimizer $\mathbf{u}^*(k)$ is the tangential point of the boundary of U_c with the level set of $J(\mathbf{x}(k), \hat{\mathbf{i}}_o(k), \mathbf{u}(k))$. Note that the input constraint region U_c represents a circle in the v_d-v_q plane, where v_d and v_q are the first and the second element of $\mathbf{u}(k)$, respectively, but the level sets of the cost function $J(\mathbf{x}(k), \hat{\mathbf{i}}_o(k), \mathbf{u}(k))$ are ellipsoids in the v_d-v_q plane. So the problem is how to find the tangential point of the boundary of U_c with the level set of $J(\mathbf{x}(k), \hat{\mathbf{i}}_o(k), \mathbf{u}(k))$. The constrained optimizer taking these points into account is summarized as Theorem 1.

Theorem 1. Assume that there exist $\beta > 0$ and $P = P^T > 0$ such that

$$B^TPB = \beta I. \quad (21)$$

Then, the optimal solution to the constrained optimization problem (19) is given by

$$\mathbf{u}^*(k) = \begin{cases} \mathbf{u}_{uc}^*(k) & \text{if } \mathbf{u}_{uc}^*(k) \in U_c, \\ \gamma^*(k)\mathbf{u}_{uc}^*(k) & \text{if } \mathbf{u}_{uc}^*(k) \notin U_c, \end{cases} \quad (22)$$

where

$$\gamma^*(k) := \frac{V_{dc}}{\sqrt{3}||\mathbf{u}_{uc}^*(k)||}. \quad (23)$$

Proof. Suppose that $\mathbf{u}_{uc}^* \notin U_c$. If the level set of the cost function (17) is a circle as well as the input constraint region U_c, the constrained optimizer to the optimization problem (19) can be obtained by finding the intersection between the boundary of the set U_c and the line segment of the two points from $\mathbf{u}(k) = \mathbf{0}$ to the unconstrained optimizer $\mathbf{u}_{uc}^*(k)$ as shown in Fig. 3 where $F(c)$ is the level set of the cost function defined by

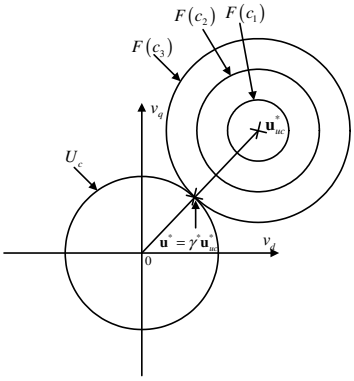

Fig. 3. Relationship between $\bar{\mathbf{u}}^*$ and $\bar{\mathbf{u}}_{uc}^*$

$$F(c) := \{\mathbf{u}(k) \mid J(\mathbf{x}(k), \hat{\mathbf{i}}_o(k), \mathbf{u}(k)) \le c\}, \ \forall c \ge 0.$$

Thanks to the assumption (21), the cost function can be written as $J(\mathbf{x}(k), \hat{\mathbf{i}}_o(k), \mathbf{u}(k))$ as

$$\begin{aligned} J(\mathbf{x}(k), \hat{\mathbf{i}}_o(k), \mathbf{u}(k)) &= (\beta + r_u)\Big(\|\mathbf{u}(k)\|^2 + 2\mathbf{u}^T(k)\mathbf{z}(k) \\ &\quad + \|\mathbf{z}(k)\|^2\Big) + \delta(k), \\ &= (\beta + r_u)\|\mathbf{u}(k) + \mathbf{z}(k)\|^2 + \delta(k) \end{aligned} \quad (24)$$

where

$$\mathbf{z}(k) := \frac{1}{\beta + r_u}\Big(B^TP\mathbf{w}(k) - r_u\hat{\mathbf{u}}^0(r,k)\Big),$$

$$\delta(k) := -(\beta + r_u)\|\mathbf{z}(k)\|^2 + \|\mathbf{w}(k)\|^2 + r_u\|\hat{\mathbf{u}}^0(r,k)\|^2.$$

It implies that the level set of the cost function (17) is a circle. If $\mathbf{u}_{uc}^*(k) \notin U_c$, the optimizer $\mathbf{u}^*(k)$ of the problem (19) is given by the point of intersection between the boundary of the set U_c and the line segment of the two points $\mathbf{u}(k) = \mathbf{0}$ and $\mathbf{u}_{uc}^*(k)$ since the level set of the cost function is a circle as well as the input constraint set U_c. Therefore, the optimizer $\mathbf{u}^*(k)$ is given as $\mathbf{u}^*(k) = \gamma^*(k)\mathbf{u}_{uc}^*(k)$ where $\gamma^*(k)$ is defined in (23).

Theorem 1 shows that the solution to the optimization problem (19) can be obtained without any use of numerical methods when the assumption (21) holds. Note that, since matrix A of the discrete time system (4) is stable, there exists $P = P^T > 0$ such that

$$A^TPA - P = -qI, \ \forall q > 0. \quad (25)$$

Actually, it can be shown that the assumption (21) holds for any matrix $P = P^T > 0$ satisfying the equation (25). Thus, the result of Theorem 1 is not restrictive since it is always possible to pick matrix P so that the assumption (21) holds.

4.3 Stability Analysis

In this section, it will be shown that $\mathbf{x}(k)$ and $\hat{\mathbf{i}}_o(k)$ converge to $\mathbf{x}^0(r,\mathbf{i}_o)$ and $\mathbf{i}_o$, respectively, using the proposed MPC method (22).

Theorem 2 proves that the closed-loop system is globally asymptotically stable by showing that the proposed MPC (22) with the DOB makes the positive definite function defined as

$$V(\mathbf{e}(k), \mathbf{e}_z(k)) := \|\mathbf{e}(k)\|_P^2 + \rho\|\mathbf{e}_z(k)\|_{P_o}^2, \quad \forall k \geq 0,\ \rho > 0,\ P_o = P_o^T > 0, \tag{26}$$

decrease monotonically. For details, see Theorem 2.

Theorem 2. Suppose that matrix P of the cost function (17) is chosen to be satisfied the inequality (25) for some $q > 0$ and that the DOB gain L_o is selected for matrix $A_{obs} = A_a - L_o C_a$ to be stable. Then, the closed-loop system with the MPC (22) and the DOB (6)-(7) is globally asymptotically stable.

By Theorem 2, it is clear that the main control objectives $\lim_{k\to\infty} \mathbf{v}_c(k) = \mathbf{v}_c^*(r)$ is successfully achieved by the proposed MPC since the errors $\mathbf{e}(k)$ and $\mathbf{e}_z(k)$ converge to zero.

4.4 Proof of zero steady-state error

Here, we show that the proposed MPC (22) eliminates the steady state error. Consider the following state values:

$$\lim_{k\to\infty} \mathbf{x}(k) = \mathbf{x}_\infty (= \begin{bmatrix} \mathbf{i}_{f,\infty} \\ \mathbf{v}_{c,\infty} \end{bmatrix}),\ \lim_{k\to\infty} \hat{\mathbf{i}}_o(k) = \hat{\mathbf{i}}_{o,\infty}, \text{ and } \lim_{k\to\infty} \mathbf{u}^*(k) = \mathbf{u}_\infty^* \in U_c. \tag{27}$$

Note that the integration effect in (7) of the DOB ensures that $\hat{\mathbf{x}}_\infty = \mathbf{x}_\infty$, where $\hat{\mathbf{x}}_\infty$ denotes the steady state of $\hat{\mathbf{x}}(k)$ of the DOB. Then, the state estimation part (6) of the DOB becomes

$$\mathbf{x}_\infty = A\mathbf{x}_\infty + B\mathbf{u}_\infty^* + B_d\hat{\mathbf{i}}_{o,\infty}, \tag{28}$$

The corresponding steady state MPC $\mathbf{u}_\infty^*$ is given by

$$\mathbf{u}_\infty^* = -(B^TPB + r_uI)^{-1}\Big(B^TP(A\mathbf{x}_\infty + B_d\hat{\mathbf{i}}_{o,\infty} - \hat{\mathbf{x}}_\infty^0(r)) - r_u\hat{\mathbf{u}}_\infty^0(r)\Big), \tag{29}$$

where

$$\hat{\mathbf{x}}_\infty^0(r) := \lim_{k\to\infty} \hat{\mathbf{x}}^0(r,k),\ \hat{\mathbf{u}}_\infty^0(r) := \lim_{k\to\infty} \hat{\mathbf{u}}^0(r,k),$$

since $\mathbf{u}_\infty^* \in U_c$. Using the equation (28), the equation (29) can be written as:

$$\mathbf{u}_\infty^* = -(B^TPB + r_uI)^{-1}\Big(B^TP(\mathbf{x}_\infty - \hat{\mathbf{x}}_\infty^0(r)) + r_u(\mathbf{u}_\infty^* - \hat{\mathbf{u}}_\infty(r))\Big) + \mathbf{u}_\infty^*.$$

It implies that

$$\Big(B^TP(\mathbf{x}_\infty - \hat{\mathbf{x}}_\infty^0(r)) + r_u(\mathbf{u}_\infty^* - \hat{\mathbf{u}}_\infty(r))\Big) = \mathbf{0}. \tag{30}$$

Now assume that matrix B has full column rank so that there exists $(B^TB)^{-1}$. Then, using the equation (28), $\mathbf{u}_\infty^*$ can be written as

$$\mathbf{u}_\infty^* = (B^TB)^{-1}B^T\Big((I-A)\mathbf{x}_\infty - B_d\hat{\mathbf{i}}_{o,\infty}\Big). \tag{31}$$

Moreover, using the definitions in (16) and (18), we have

$$\hat{\mathbf{x}}_\infty^0(r) = A\hat{\mathbf{x}}_\infty^0(r) + B\hat{\mathbf{u}}_\infty^0(r) + B_d\hat{\mathbf{i}}_{o,\infty},$$

where

$$\hat{\mathbf{u}}_\infty^0(r) = (B^TB)^{-1}B^T\Big((I-A)\hat{\mathbf{x}}_\infty(r) - B_d\hat{\mathbf{i}}_{o,\infty}\Big), \tag{32}$$

$\hat{\mathbf{x}}_\infty^0(r) := \begin{bmatrix} \hat{\mathbf{i}}_{f,\infty}^0(r) & \mathbf{v}_c^*(r) \end{bmatrix}^T$. Subtracting (32) from (31), the equation (30) can be expressed as

$$\Big(B^TP + r_u(B^TB)^{-1}B^T(I-A)\Big)(\mathbf{x}_\infty - \hat{\mathbf{x}}_\infty^0(r)) = \mathbf{0} \tag{33}$$

It follows from the relations (16) and (18) that

$$(F_1Z_{11} + F_2)(\mathbf{v}_{c,\infty} - \mathbf{v}_c^*(r)) = \mathbf{0}, \tag{34}$$

where

$$F = [\,F_1\ \ F_2\,] := B^TP + r_u(B^TB)^{-1}B^T(I-A).$$

Thus, the equation (34) implies that the proposed MPC rejects steady-state errors if matrix $F_1Z_{11} + F_2$ is invertible. The following two sections evaluate the closed-loop performance using the MPC (22) through simulations and experiments.

5. EXPERIMENTS

In this experiments, the parameters of the three phase UPS system are given by

$$R = 0.1\Omega,\ L = 1.3\text{mH},\ C = 20\mu\text{F},\ \omega = 120\pi,\ V_{dc} = 450V.$$

For PWM (pulse width modulation), the switching frequency is chosen as $10kHz$. The proposed MPC is implemented by using the digital signal processor TMS320F28335 with the sampling time of $h = 0.1ms$. The control weight r_u of the cost function (17) is set to be $r_u = 0.2$. First, the closed-loop performance is shown with the use of resistive load $R_L = 35\Omega$ and the output voltage reference $r = 156V$, which means $156V$ in root mean square (RMS). Fig. 5 depicts the voltage regulation performance with the output current behavior in the a-b-c frame. The corresponding the

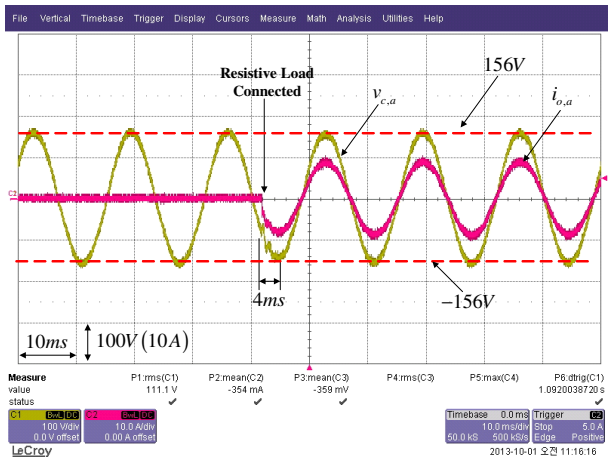

Fig. 4. The a-frame output voltage ($v_{c,a}$) and the a-frame output current responses for the voltage reference $r = 156V$

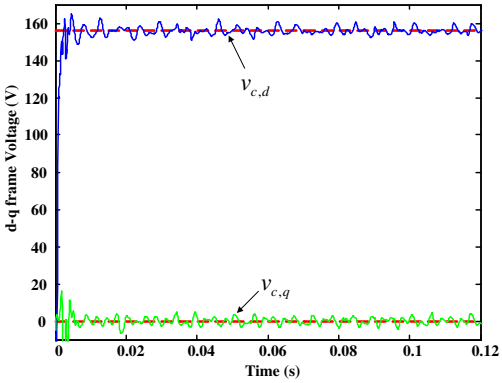

Fig. 5. Voltage tracking performance in the d-q frame

output voltage responses is depicted in Fig. 5. In Fig. 6, the steady-state voltage, output current responses, and the corresponding voltage total harmonic distortion (THD) analysis results are presented. These results show that there is no steady-state error in the the output voltage and that the corresponding THD value is satisfactory (1.2%) with respect to a resistive load.

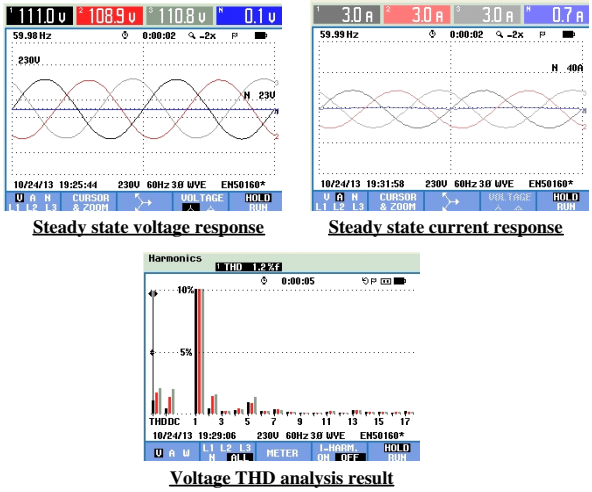

Fig. 6. Steady-state voltage and current responses with the voltage THD analysis result (resistive load)

6. CONCLUSIONS

In this paper, an offset-free MPC scheme is presented. The proposed MPC minimizes the one step ahead cost function by performing a simple membership test while the DOB estimates the disturbance; any numerical methods and any off-line optimization such as partitioning the state space are not required. Besides, it is shown that the closed-loop system is globally asymptotically stable in the presence of input constraints and that the integral action in the DOB eliminates the steady state errors caused by a model-plant mismatch. The effectiveness of the proposed MPC is experimentally shown using a resistive load.

REFERENCES

N. M. Abdel-Rahim and J. E. Quaicoe. Analysis and design of a multiple feedback loop control strategy for single-phase voltage-source UPS inverters. *IEEE Trans. Power Electron.*, 11:532–541, 1996.

A. Bemporad, F. Borrelli, and M. Morari. Model predictive control based on linear programming; the explicit solution. *IEEE Trans. Autom. Control*, 47:1974–1985, 2002.

F. Borrelli. *Constrained Optimal Control of Linear and Hybrid Systems*. New York: Springer-Verlag, 2003.

J.-S. Cho, S.-Y. Lee, H.-S. Mok, and G.-H. Choe. Modified deadbeat digital controller for UPS with 3-phase PWM inverter. In *Industry Applications Conference, Thirty-Fourth IAS Annual Meeting*, 2012.

P. Cortes, G. Ortiz, J. I. Yuz, J. Rodriguez, S. Vazquez, and L. G. Franquelo. Model predictive control of an inverter with output LC filter for UPS applications. *IEEE Trans. Ind. Electron.*, 56:1875–1883, 2009.

P. Cortes, J. Rodriguez, S. Vazquez, , and L. G. Franquelo. Predictive control of a three-phase UPS inverter using two steps prediction horizon. In *2010 IEEE International Conference on Industrial Technology (ICIT)*, 2010.

Y. Ito and S. Kawauchi. Microprocessor-based robust digital control for UPS with three-phase PWM inverter. *IEEE Trans. Power Electron.*, 10:196–204, 1995.

J. C. Kassakian, M. Schlecht, and G. C. Verghese. *Principles of power electronics*. MA: Addison-Wesley, 1991.

T. Kawabata, T. Miyashita, and Y. Yamamoto. Deadbeat control of three phase PWM inverter. *IEEE Trans. Power Electron.*, 5:21–28, 1990.

S.-K Kim, C.R.Park, and Y.I.Lee. One-step ahead model predictive controller of three-phase inverter for uninterruptible power supply applications. In *Proceedings of Applied Power Electronics Conference and Exposition*, 2014.

T.S. Lee, S.-J. Chiang, and J.-M. Chang. H_∞ loop-shaping controller designs for the single-phase UPS inverters. *IEEE Trans. Power Electron.*, 54:1591–1602, 2001a.

T.S. Lee, K.S. Tzeng, and M.S. Chong. Robust controller design for a single-phase UPS inverter using μ-synthesis. *IEEE Trans. Power Electron.*, 54:1591–1602, 2001b.

Jae Sik Lim and Young Il Lee. Design of a robust controller for three-phase UPS systems using LMI approach. In *2012 International Symposium on Power Electronics, Electrical Drives, Automation and Motion (SPEEDAM)*, 2012.

P. C. Loh, M. J. Newman, D. N. Zmood, and D. G. Holmes. A comparative analysis of multiloop voltage regulation strategies for single and three-phase UPS systems. *IEEE Trans. Power Electron.*, 18:1176–1185, 2003.

S. Mariethoz and M. Morari. Explicit model-predictive control of a PWM inverter with an LCL filter. *IEEE Trans. Ind. Electron.*, 56:389–399, 2009.

N. Mohan, T. M. Undeland, and W. P. Robbins. *Power Electronics: Converters, Applications, and Design*. NJ: Wiley, 1995.

R. Vargas, P. Cortes, U. Ammann, J. Rodriguez, and J. Pontt. Predictive control of a three-phase neutral-point-clamped inverter. *IEEE Trans. Ind. Electron.*, 54: 2697–2705, 2007.

G. Willmann, D. F. Coutinho, L. F. A. Pereira, and F. B. Libano. Multiple-loop H_∞ control design for uninterruptible power supplies. *IEEE Trans. Ind. Electron.*, 54:1591–1602, 2007.